JOURNAL OF SOLID STATE CHEMISTRY 119, 134–141 (1995)

# The Calcium Thallate $Ca_3Tl_4O_9$, an Intergrowth of the $CaTl_2O_4$ and $Ca_2Tl_2O_5$ Structures, Member $n = 1.5$ of the Series $Ca_nTl_2O_{n+3}$

F. Goutenoire, V. Caignaert, M. Hervieu, and B. Raveau

*Laboratoire CRISMAT-CNRS URA 1318-ISMRA, Université de Caen, Boulevard du maréchal Juin, 14050 Caen Cedex, France*

Received December 2, 1994; in revised form March 13, 1995; accepted March 15, 1995

**A new calcium thallate $Ca_3Tl_4O_9$ has been isolated. It crystallizes in a monoclinic cell, space group $C2/m$, with $a = 11.118(3)$ Å, $b = 3.341(1)$ Å, $c = 12.287(3)$ Å, and $\beta = 102.88(2)°$. The ab initio determination of this strucure shows that it consists of a regular intergrowth of the first two members of the calcium thallate family $Ca_nTl_2O_{3+n}$: $CaTl_2O_4$ ($n = 1$) and $Ca_2Tl_2O_5$ ($n = 2$). Intergrowth defects have been characterized by electron microscopy. Among all oxides and sulfides that belong to the lillianite family, $Ca_3Tl_4O_9$ is the only one that exhibits the $^{2,3}$L structure, i.e., where layers are built up from ribbons of two and three edge-sharing octahedra alternately.** © 1995 Academic Press, Inc.

## INTRODUCTION

The recent exploration of the system Ca–Tl–O (1, 2) has allowed a new series of oxides $Ca_nTl_2O_{3+n}$ to be isolated, whose structure is closely related to the rock salt family. These thallates exhibit indeed zigzag rock salt layers sharing the corners of their octahedra and forming quasi-triangular tunnels, occupied by calcium. The first two members $CaTl_2O_4$ (1) and $Ca_2Tl_2O_5$ (1) can be described as chemical twinning of the rock salt structure. The $n = 1$ member, which is in fact isotypic with $CaTi_2O_4$ (3), consists of $[Tl_2O_4]_\infty$ layers built up of double ribbons of edge-sharing $TlO_6$ octahedra (Fig. 1a). The second member, $Ca_2Tl_2O_5$, is derived from the first one, by increasing the thickness of the rock salt layers, that is, by replacing double octahedral ribbons by triple ribbons, so that $[CaTl_2O_5]_\infty$ layers are formed (Fig. 1b). The third member of this series $Ca_3Tl_2O_6$ (2), isostructural with $Ca_3In_2O_6$ (4), forms $[Ca_2Tl_2O_6]_\infty$ rock salt layers built up from quadruple octahedral ribbons (Fig. 1c), but differs from the first two members by the absence of chemical twinning. In fact, these oxides are closely related to the lead, bismuth, and silver sulfides of the lillianite homologous series whose crystal chemistry was extensively studied by Makovicky *et al.* (5–7) and Takagi *et al.* (8, 9). Contrary to the sulfides, very few oxides belong to this family since, besides these recently discovered thallium oxides, only one compound $CaTi_2O_4$ (3) is member of this series. Thus, the recent results concerning the Ca–Tl–O system show the great ability of trivalent thallium to form octahedral ribbons and suggest that it should be possible to synthesize other members of the series. The present work deals with a new thallate, $Ca_3Tl_4O_9$, member $n = 1.5$ of the $Ca_nTl_2O_{3+n}$ series, whose original structure corresponds to an intergrowth of the first two members and has not previously been observed, either for oxides or for sulfides.

## EXPERIMENTAL

The oxide $Ca_3Tl_4O_9$ was prepared from mixtures of $Tl_2O_3$ and CaO, varying the Tl/Ca ratio from 1.3 to 1.6. The weighed powders were mixed in an agate mortar. The mixtures were placed in alumina crucibles and sealed in evacuated silica tubes. The different tubes were heated progressively to 750°C for 48 hr and then slowly cooled to room temperature. The final products are brown.

The powder X-ray pattern of the new phase was registered with a Bragg–Brentano diffractometer; the details of the collection are presented in Table 1. The X-ray pattern was used to refine the structure with the profile program Fullprof (10).

The electron diffraction study of the microcrystals was performed with a JEOL 200CX electron microscope fitted with an eucentric goniometer (±60°) and equipped with an energy dispersive X-ray spectrometry (EDS) analyzer.

## RESULTS AND DISCUSSION

Under the above conditions, a new phase is obtained for nominal compositions ranging from $CaTl_{1.4}O_{3.1}$ to $CaTl_{1.6}O_{3.4}$, in the form of a well-crystallized brown powder. The EDS analysis, performed on more than 30 microcrystals in the sample with nominal composition $CaTl_{1.5}O_{3.25}$, leads to an atomic ratio $Tl/Ca = 1.35 \pm 0.05$; this result shows that bulk composition remains constant from one grain to another and suggests that a small Tl loss occurs during the synthesis. Thus the ideal composition $Ca_3Tl_4O_9$ can be proposed for this new phase. The electron



0022-4596/95 $12.00

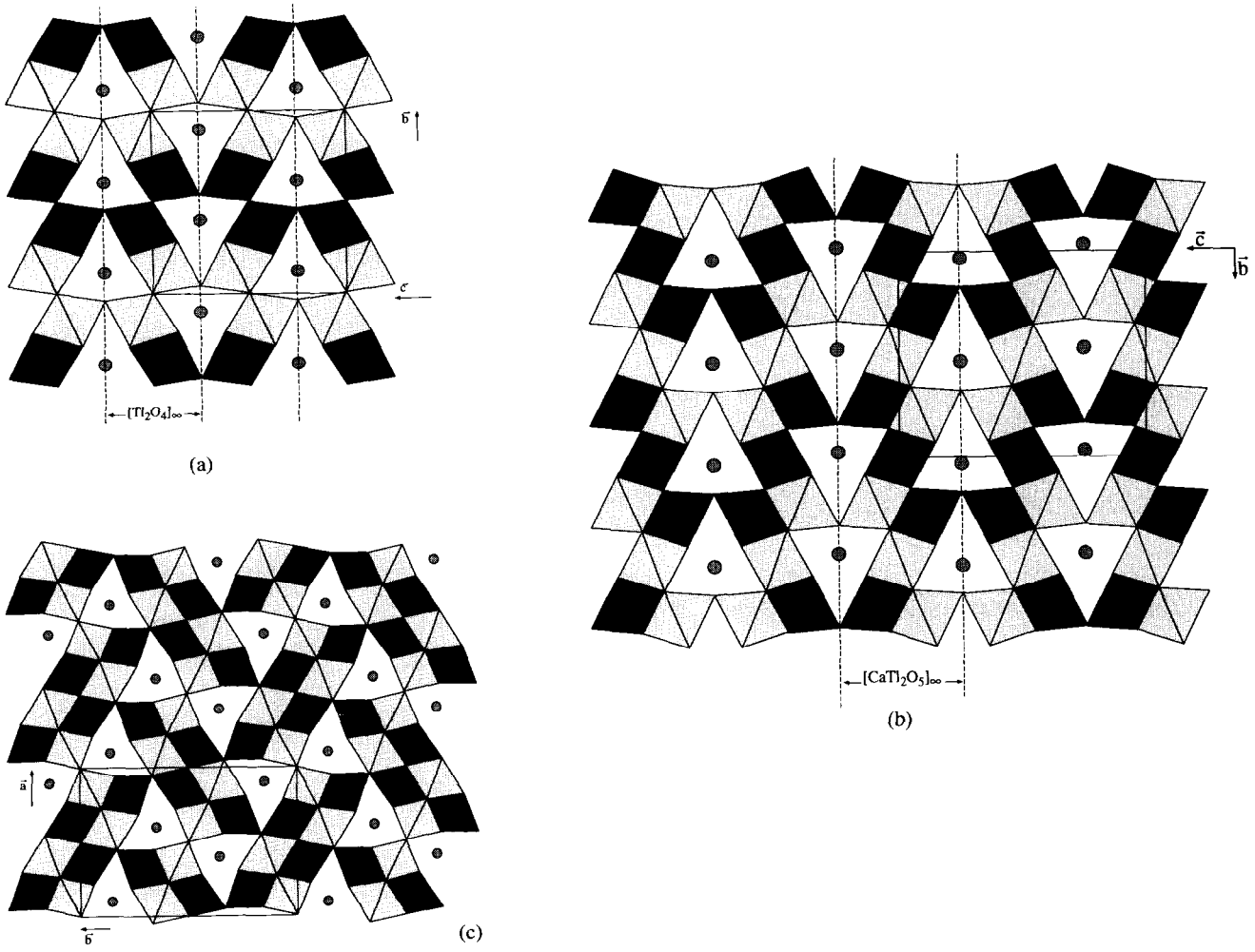


FIG. 1. (a) Projection of the $CaTl_2O_4$ structure onto (001) plane. The thallium octahedra (light grey and dark grey) are shifted by **c**/2 with respect to each other. (b) Projection of the $Ca_2Tl_2O_5$ structure onto (001) plane. Dark grey and light grey octahedra are shifted by **c**/2. (c) Projection of the $Ca_3Tl_2O_6$ structure onto (001) plane. Dark grey and light grey octahedra are shifted by **c**/2.

TABLE 1
**Rietveld Refinement Data for $Ca_3Tl_4O_9$**

| | |
|---|---|
| Diffractometer | Seifert |
| Radiation | *CuKα1*, ($SiO_2$ ($10\bar{1}1$) primary monochromator) |
| $2\theta$ range [°] | 14–120 acquisition, 25–120 for refinement |
| Step-scan increment [°] | 0.02 |
| Count time [sec/step] | 15 |
| Peak shape | Pseudo-Voigt |
| Number of observations | 5300 |
| Number of reflexion | 400 |
| Number of refined structural parameters | 20 + 1 (preferred orientation) |
| Number of profile parameters | 9 |
| $R_i$ | 9.36% |
| $R_p$ | 15.1% |
| $R_{wp}$ | 18.3% |
| $R_{exp}$ | 11.55% |
| $\chi^2$ | 2.51% |

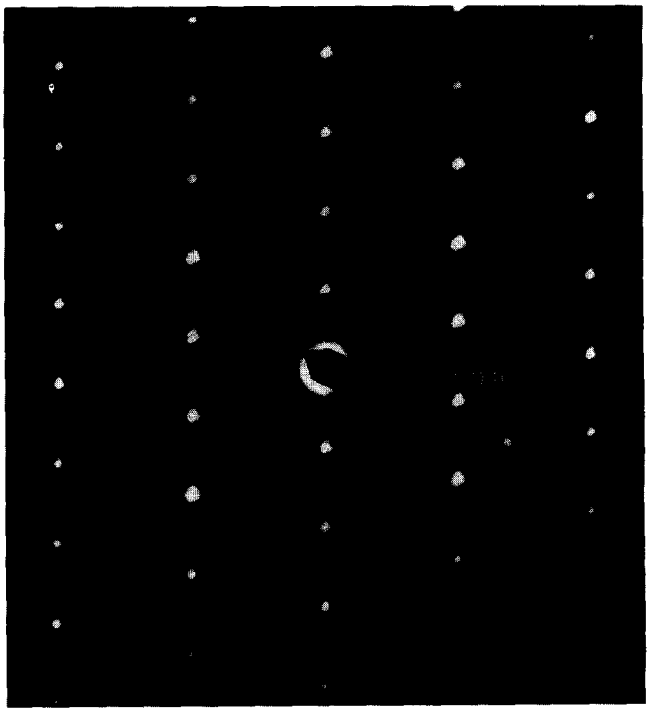

FIG. 2. [010] ED pattern of $Ca_3Tl_4O_9$.

diffraction (ED) study (Fig. 2) shows a monoclinic cell, with the condition-limiting reflections $hkl$, $h + k = 2n$, corresponding to the possible space groups $C2/m$, $C2$, or $Cm$. The cell parameters found by the autoindexing program TREOR (11) with the data of the X-ray pattern, based on the first 20 Bragg reflections, confirm the monoclinic symmetry with the parameters $a = 11.11$ Å, $b = 3.341$ Å, $c = 12.28$ Å, $\beta = 102.8°$, with a merit factor $M(20) \approx 21$ (12). The cell parameters were finally refined with the Fullprof program (10) to $a = 11.118(3)$ Å, $b = 3.341(1)$ Å, $c = 12.287(3)$ Å, and $\beta = 102.88(2)°$. (See Fig. 3.)

At this stage of the investigation, the values of the cell parameters suggest that this new phase corresponds to the intergrowth of the two members $CaTl_2O_4$ ($n = 1$) and $Ca_2Tl_2O_5$ ($n = 2$). Two structural models can be proposed for such an intergrowth. The first one (Fig. 4a) is built up from alternating $[CaTl_2O_5]_\infty$ and $[Tl_2O_4]_\infty$ layers in which all the tunnels are similar since they are all bordered by one $n = 1$ and one $n = 2$ layer. In the second model (Fig. 4b), two $[CaTl_2O_5]_\infty$ adjacent layers alternate with two $[Tl_2O_4]_\infty$ layers so that three types of tunnels are formed; the first one is bordered by $[CaTl_2O_5]_\infty$ layers only, the second one is bordered by $[Tl_2O_4]_\infty$ layers only, as in $Ca_2Tl_2O_5$ and $CaTl_2O_4$, respectively, and the third type results from the assemblage of one $[Tl_2O_4]_\infty$ layer with

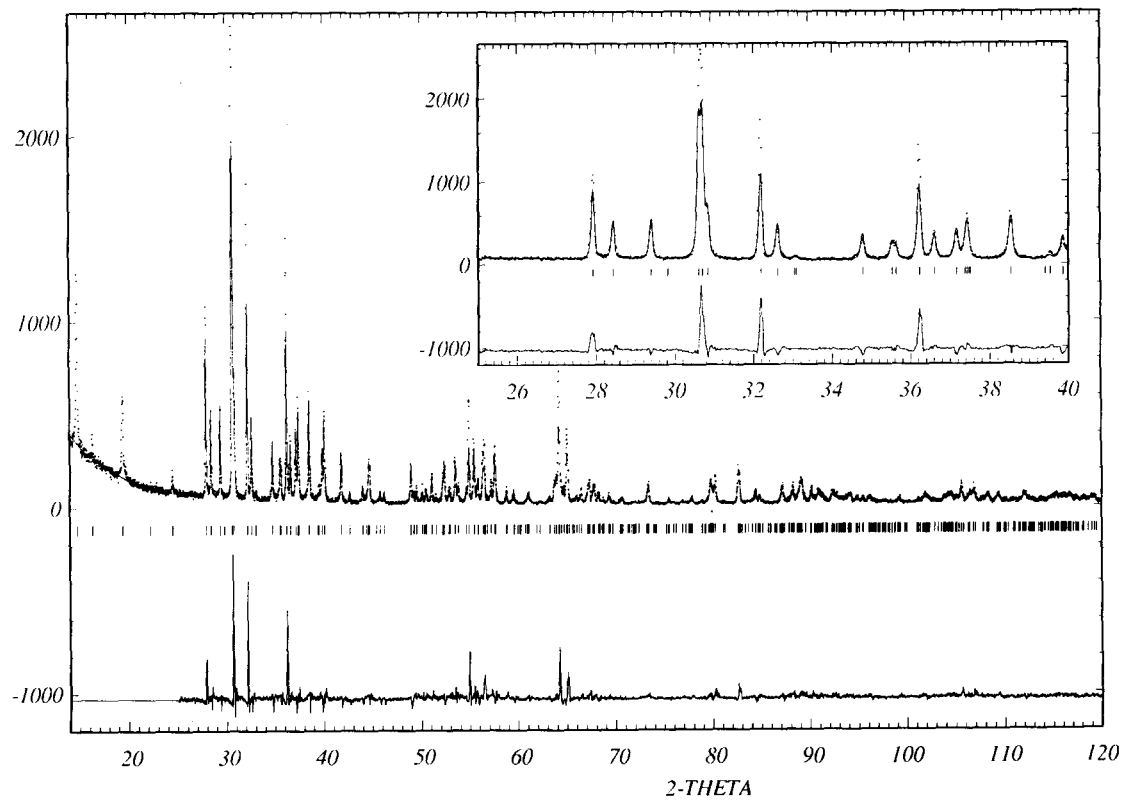


FIG. 3. Final profile refinement of the XRD pattern of $Ca_3Tl_4O_9$. Observed (point), calculated (line), and difference (lower) profiles are shown.

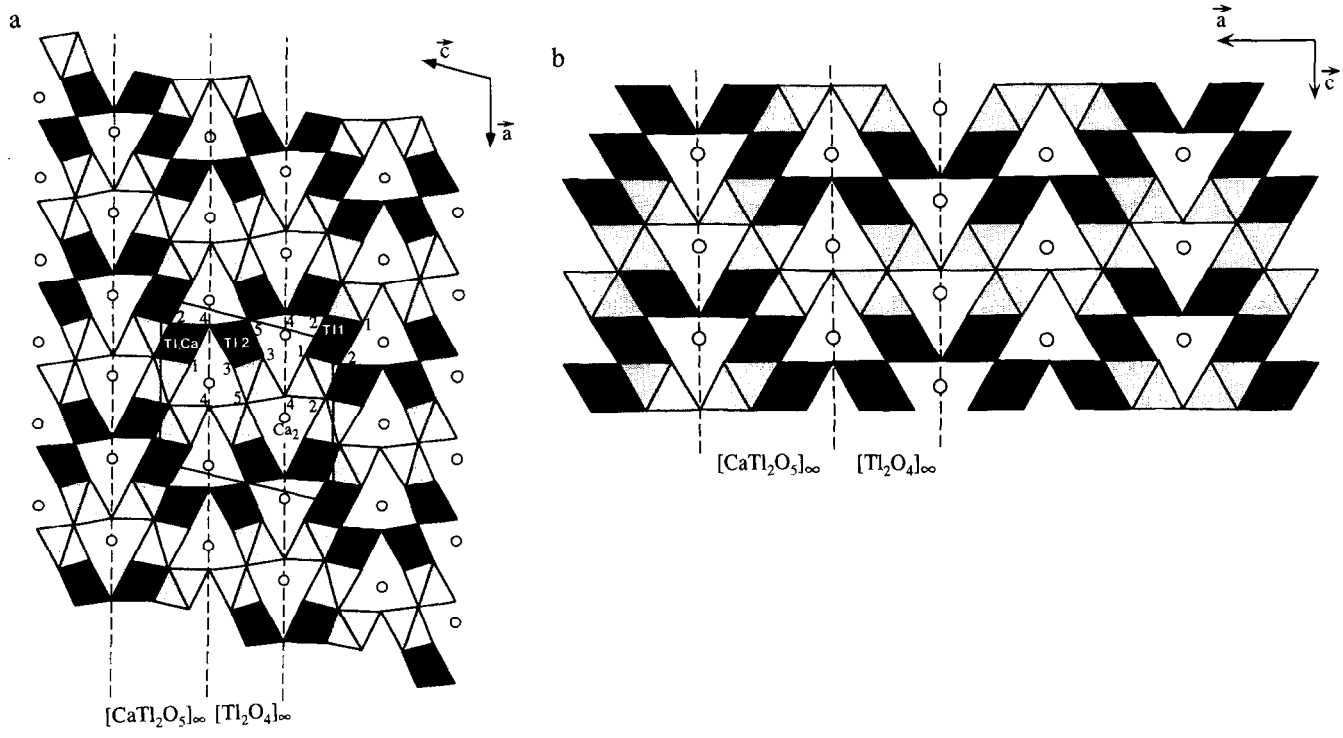


FIG. 4. Projection of two possible structural models for $Ca_3Tl_4O_9$ onto (010) plane. (a) Model I (actual structure): one $[CaTl_2O_5]_\infty$ layer alternates with one $[Tl_2O_4]_\infty$ layer. (b) Model II (not observed): two $[Tl_2O_4]_\infty$ layers alternate with two $[CaTl_2O_5]_\infty$ layers.

one $[CaTl_2O_5]_\infty$ layer. The cell symmetry is in favor of the first model. This hypothesis is strongly supported by electron microscopy observations, although only low-resolution images could be obtained due to the preferential orientation of the crystals. The low-resolution images (Fig. 5) exhibit bright fringes regularly spaced by 5.3 and 6.8 Å along **c** alternately according to sequence "5.3–6.8," which corresponds to the spacing of the (001) calcium layers in the first structural model (Fig. 4a), whereas the second model (Fig. 4b) would involve the sequence "5.3–5.3–6.8–6.8."

The ab initio resolution of the structure was carried out by the heavy atom method, in the centrosymmetric space group $C2/m$. The integrated intensities are extracted from

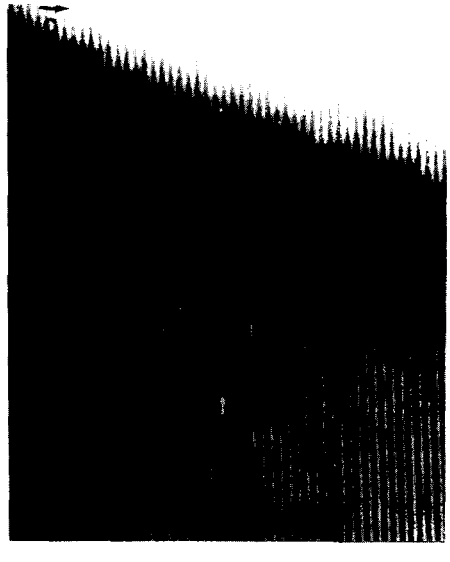

FIG. 5. Low-resolution image of a $Ca_3Tl_4O_9$ crystal: the bright fringes are regularly spaced by 5.3 and 6.8 Å along **c**.

TABLE 2
**Crystallographic Parameters of $Ca_3Tl_4O_9$**

| Atom | Site | $x$ | $y$ | $z$ | Occupancy | $B$ (Å$^2$) |
|---|---|---|---|---|---|---|
| Tl1 | 2*a* | 0.0 | 0.0 | 0.0 | 1 | 0.43 |
| Tl2 | 4*i* | 0.1505(2) | 0.0 | 0.5632(2) | 1 | 0.26(6) |
| Ca1 | 4*i* | 0.2383(4) | 0.0 | 0.8707(6) | 0.53(1) | 0.1(1) |
| Tl3 | 4*i* | | | | 0.47(1) | |
| Ca2 | 4*i* | 0.5499(9) | 0.0 | 0.289(1) | 1 | 0.5[a] |
| O1 | 4*i* | 0.127(3) | 0.0 | 0.159(3) | 1 | 0.5[a] |
| O2 | 4*i* | 0.369(3) | 0.0 | 0.044(3) | 1 | 0.5[a] |
| O3 | 4*i* | 0.198(3) | 0.0 | 0.390(3) | 1 | 0.5[a] |
| O4 | 4*i* | 0.098(3) | 0.0 | 0.720(2) | 1 | 0.5[a] |
| O5 | 2*d* | 0.5 | 0.0 | 0.5 | 1 | 0.5[a] |

*Note*: Space group: $C2/m$, $z = 2$; cell parameters: $a = 11.118(3)$ Å, $b = 3.341(1)$ Å, $c = 12.287(3)$ Å, $\beta = 102.88(2)°$.

[a] $B$ for oxygen atom are arbitrarily fixed to 0.5 Å$^2$.

TABLE 3
Interatomic Distances for $Ca_3Tl_4O_9$ in Å

| | | |
|---|---|---|
| Tl1–O1 | 2.15(3) | (2×) |
| Tl1–O2 | 2.35(3) | (4×) |
| Tl2–O3 | 2.30(4) | (1×) |
| Tl2–O3 | 2.35(2) | (2×) |
| Tl2–O4 | 2.13(4) | (1×) |
| Tl2–O5 | 2.37(2) | (2×) |
| Ca1/Tl3–O1 | 2.32(3) | (2×) |
| Ca1/Tl3–O2 | 2.30(3) | (1×) |
| Ca1/Tl3–O2 | 2.42(3) | (2×) |
| Ca1/Tl3–O4 | 2.13(3) | (1×) |
| Ca2–O1 | 2.59(3) | (2×) |
| Ca2–O3 | 2.47(3) | (2×) |
| Ca2–O4 | 2.33(3) | (2×) |
| Ca2–O5 | 2.76(2) | (1×) |

the powder X-ray data corresponding to the range $14° \leq 2\theta \leq 70°$ by a full pattern decomposition method with the Fullprof program. As for $Ca_2Tl_2O_5$ (1), the resolution of the Patterson function is complex, due to a mixed site occupied half by calcium and half by thallium, leading to (Tl–Ca) peaks corresponding to different sites. The positions of the thallium (Tl1) and Tl2) formed the initial model for the Rietveld refinements using the Fullprof program. The mixed Tl/Ca sites are located after subsequent cycles of refinement and difference Fourier syntheses. The final cationic sites refinement gave a ratio Tl/Ca ≈ $\frac{4}{3}$, in agreement with the EDS analyses. The oxygen sites are found following the same process. The atomic coordinates of all the atoms, the occupancy factors of the metallic sites, and the isotropic thermal factor $B$ of the metallic atoms are refined successively, the thermal factor $B$ of oxygen being arbitrarily fixed at $B = 0.5$ Å$^2$ due to its low scattering power. The final atomic parameters (Table 2) correspond to a reliability factor $R_i = 0.093$, whose rather high value is explained below.

These results show that $Ca_3Tl_4O_9$ corresponds to a regular intergrowth of the two structures $CaTl_2O_4$ (1) and $Ca_2Tl_2O_5$ (1) in such a way that one $[Tl_2O_4]_\infty$ layer parallel to (001) alternates with one $[Ca_2Tl_2O_5]_\infty$ layer along **c**, two successive layers sharing the corners of their octahedra (Fig. 4a). As in $CaTl_2O_4$ (1), each $[Tl_2O_4]_\infty$ layer consists of double octahedral chains of edge-sharing octahedra located at the same level (e.g., light grey in Fig. 4a) that share their edges with identical double chains of edge-sharing octahedra but shifted by **b**/2 (e.g., dark grey in Fig. 4a). In the same way, each $[CaTl_2O_5]_\infty$ layer is built up from triple chains of edge-sharing octahedra at the same level $y$ (e.g., light grey in Fig. 4a) that share their edges with identical chains of edge-sharing octahedra but shifted by **b**/2 (e.g., dark grey in Fig. 4a). In each triple chain, the central chain is occupied by thallium only, whereas the two other chains are occupied half by thallium and half by calcium. Such a mixed occupancy can be the

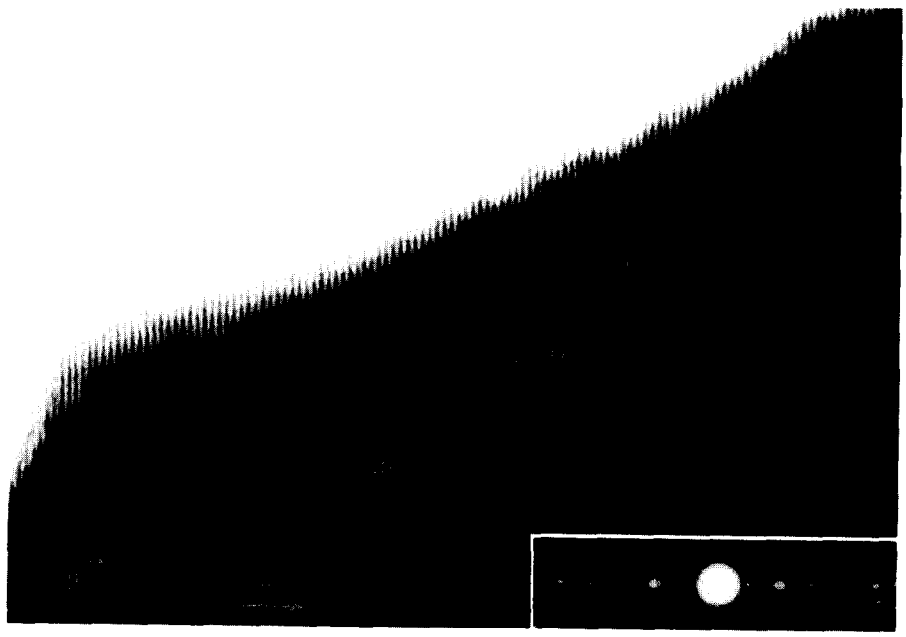

FIG. 6. Low-resolution image and ED pattern of a defective $Ca_3Tl_4O_9$ crystal: streaks are observed along **c***; the interfringe distances show that two $n = 1$ (white arrows) or two $n = 2$ (black arrows) members are, locally, adjacent.

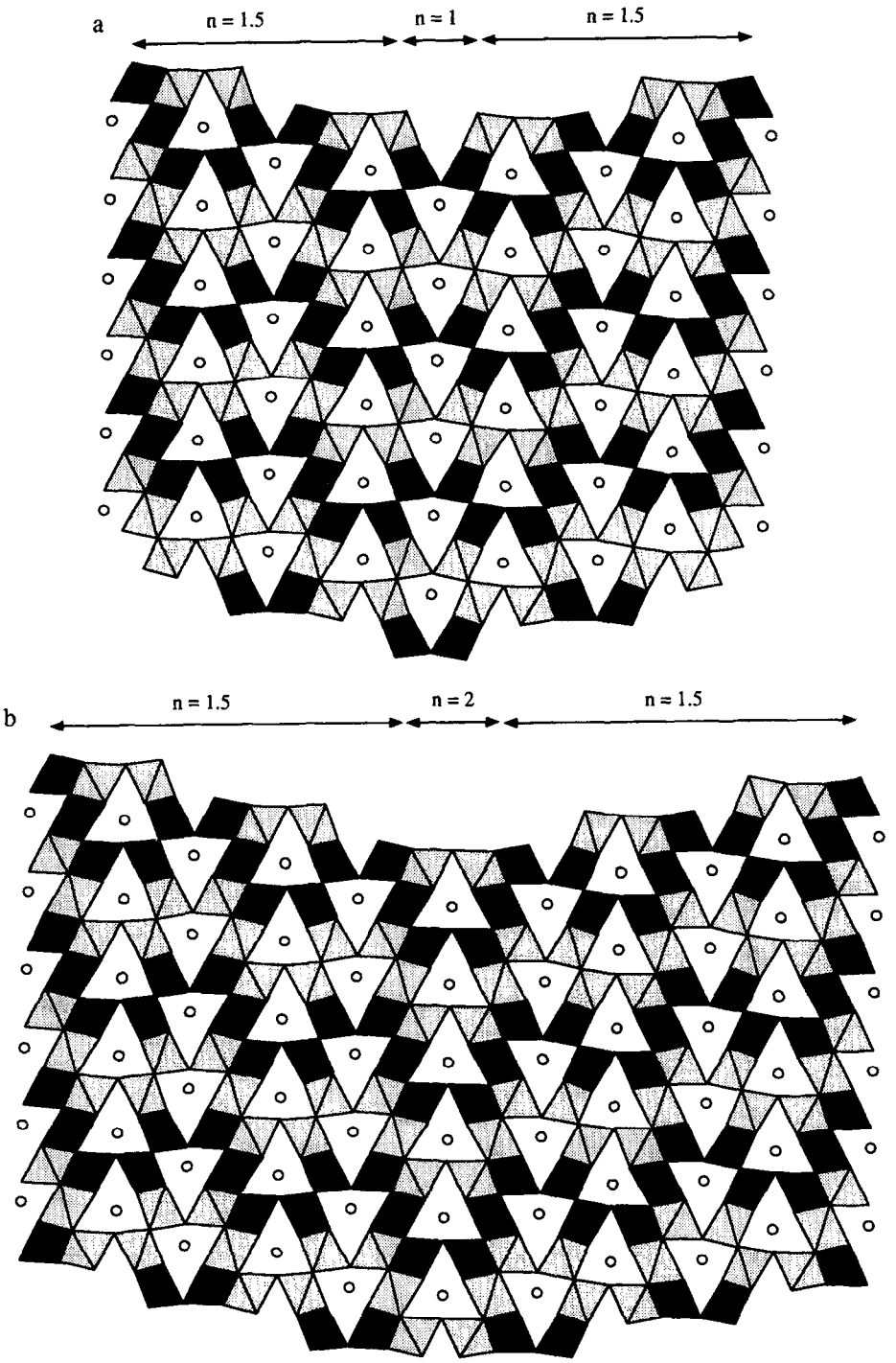


FIG. 7. Structural models showing: (a) a "$n$ = 1" defect in the "$n$ = 1.5" matrix of $Ca_3Tl_4O_9$. (b) a "$n$ = 2" defect in the "$n$ = 1.5" matrix of $Ca_3Tl_4O_9$.

result of a statistical distribution of Ca and Tl in the site 4*i* of the centrosymmetric space group $C2/m$; however, an ordered distribution could be considered with the existence of a calcium site 2*a* and a thallium site 2*a* in the noncentrosymmetric group $Cm$. The refinement of the positional parameters and the occupancies of the two sites do not provide any significant decrease of Ri factor, suggesting a model with a statistical distribution.

Due to the rather high reliability factor, this average structure cannot be considered to be very accurate. Nev-

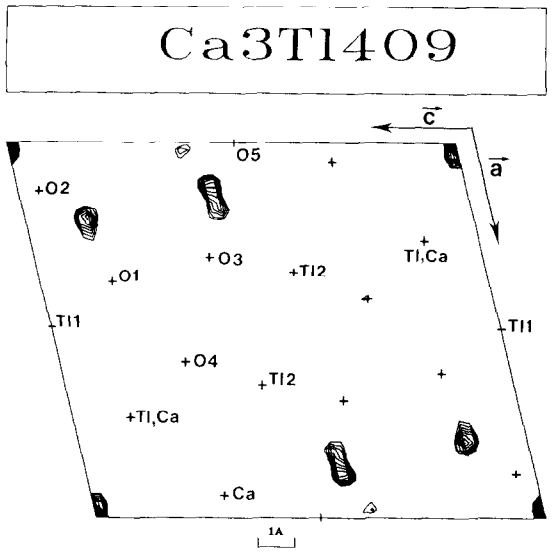


FIG. 8. Fourier difference map after the refinement of the atomic positions. Section at $y = \frac{1}{2}$ in the $(x, z)$ plane (the positions of atoms at $y = \frac{1}{2}$ are marked).

ertheless the interatomic distances can be considered as significant and are in agreement with the ionic radii of the elements (13). Note that the Tl–O distances and (Ca/Tl)–O distances (Table 3) ranging from 2.13 to 2.42 Å are very similar to those observed for $CaTl_2O_4$ (2.14 to 2.44 Å) and $Ca_2Tl_2O_5$ (2.09 to 2.42 Å). They are slightly different from those observed for $Ca_3Tl_2O_6$ that exhibits Tl–O distances ranging from 2.06 to 2.64 Å and (Ca/Tl)–O distances ranging from 2.32 to 2.55 Å. On the opposite, one observes a monocapped trigonal prismatic coordination for the calcium atoms located in the tunnels with six Ca–O distances ranging from 2.33 to 2.59 Å and a seventh oxygen further apart (2.76 Å). In this respect $Ca_3Tl_4O_9$ is close to $Ca_3Tl_2O_6$, for which a monocapped trigonal prism $CaO_7$ with six Ca–O distances ranging from 2.43 to 2.46 Å and a longer one of 2.68 Å is observed. On the other hand, one observes a pure trigonal prismatic coordination for calcium in $Ca_2Tl_2O_5$ with Ca–O distances ranging from 2.27 to 2.51 Å, whereas a bicapped trigonal prismatic coordination of calcium is observed in $CaTl_2O_4$ with six Ca–O distances ranging from 2.32 to 2.39 Å and two longer distances of 2.87 Å.

In order to explain the rather high reliability factor, a systematic investigation of the crystals has been carried out by electron diffraction and electron microscopy, recording ED patterns for numerous microcrystals; it appears that some crystals exhibit elongated reflections along **c*** and even streaks (Fig. 6), which suggest the presence of intergrowth defects. The corresponding low-resolution images (Fig. 6) confirm this hypothesis. One indeed observes series of double bright fringes spaced by 5.3 Å (white arrows) and by 6.8 Å (black arrows) instead of regular sequence "5.3–6.8," characteristic of the $Ca_3Tl_4O_9$ matrix. Such defects correspond to the local matrix of two adjacent $n = 1$ (Fig. 7a) and $n = 2$ (Fig. 7b) members, respectively. They can be interpreted by the presence of a (100) mirror at $00\frac{1}{4}$ and $00\frac{3}{4}$. These defects may be partly responsible for some significant differences observed between $I_{obs}$ and $I_{calc}$ in the XRD pattern (Fig. 3). Nevertheless they cannot explain the Fourier difference map (Fig. 8) that shows a significant electron density in the (010) plane at $y = \frac{1}{2}$. The latter phenomena suggest that, locally, a similar cationic arrangement may exist, but translated by **b**/2. Consequently such defects cannot be detected by low-resolution electron microscopy. Unfortunately the quality of the crystals and their low stability under the electronic beam do not allow this model to be checked by high-resolution electron microscopy.

## CONCLUDING REMARKS

The oxide $Ca_3Tl_4O_9$ represents the first intergrowth that has been synthesized until now in the series $Ca_nTl_2O_{3+n}$. In a more general way, the behavior of the system Ca–Tl–O can be considered as rather exceptional, since it is one of the rare oxide systems that exhibits compounds belonging to the sulphide Lillianite family. This very large family of sulphides reviewed by Makovicky *et al.* (5–7) consists indeed of different members which can be classified by the formalism $^{N1,N2}L$, where $N1$ and $N2$ represent the number of edge-sharing octahedra that characterize the ribbons forming each octahedral layer ($L$). Many sulfides with $N = N1 = N2 = 1, 2, 4, 5, 9, 11$ are known, such as for instance $^{1,1}L$ ($NdYbS_3$) (14), $^{4,4}L$ lillianite ($Pb_3Bi_2S_6$) (15), and $^{7,7}L$ heyrovskite (9, 15, 16). Sulfides with $N1 \neq N2$ such as $^{4,7}L$ vikingite (7) and $^{4,8}L$ treasurite have been also synthesized. Among all oxides and sulfides that belong to the lillianite family, $Ca_2Tl_2O_5$ (1) and $Ca_3Tl_4O_9$ are to our knowledge the only compounds that exhibit the $^{3,3}L$ and $^{2,3}L$ structures, respectively.

## REFERENCES

1. F. Goutenoire, V. Caignaert, M. Hervieu, C. Michel, and B. Raveau, *J. Solid State Chem*, in press.
2. F. Goutenoire, V. Caignaert, M. Hervieu, and B. Raveau, *J. Solid State Chem.*, in press.
3. E. F. Bertaut and P. Blum, *Acta Crystallogr. Sect. A* **12** 121 (1956).
4. R. V. Schenck and H. K. Müller-Buschbaum, *Z. Anorg. Chem.* **335** 30 (1967).
5. E. Makovicky, *Eur. J. Mineral.* **5**, 545 (1993).
6. E. Makovicky and S. Korup-Møller, *N. Jb. Miner. Abh.* **130**(3) 264 (1977).

7. E. Makovicky, M. G. Mumme, and I. C. Madsen, *N. Jb. Miner. Abh.* 454 (1992).
8. J. Takagi and Y. Takeuchi, *Acta Crystallogr. Sect. B* **28,** 649 (1972).
9. Y. Takeuchi and J. Takagi, *Proc. Jpn. Acad.* **50,** 76 (1974).
10. J. Rodriguez-Carvajal, *in* "Satellite Meeting on Powder Diffraction, Abstract on the XVth Conference of the International Union of Crystallography (Toulouse, 1990)." p. 127.
11. P. E. Werner, *Z. Kristallogr.* **120,** 375 (1964).
12. P. M. De-Wolff, *J. Appl. Crystallogr.* **1,** 108 (1968).
13. R. D. Shannon, *Acta Crystallogr. Sect. A* **32** 751 (1976).
14. D. Carre and P. Laruelle, *Acta Crystallogr. Sect. B.* **30,** 952 (1974).
15. H. H. Otto and H. S. Stunz, *N. Jb. Miner. Abh.* **108,** 1 (1968).
16. A. Skowron and J. D. Tilley, *J. Solid State Chem.* **85,** 235 (1990).